

# Preparation and Characterization of Spherical Calcium Hydroxyapatite

Kazuhiko Kandori,\* Akemi Yasukawa, and Tatsuo Ishikawa

School of Chemistry, Osaka University of Education, Asahigaoka 4-698-1,  
Kashiwara-shi, Osaka 582, Japan

Received May 24, 1994. Revised Manuscript Received October 13, 1994<sup>⊗</sup>

The preparation of spherical calcium phosphate particles by aging a solution containing  $\text{CaSO}_4$  and  $\text{NaH}_2\text{PO}_4$  at 80 and 100 °C in the presence of urea (1 mol/dm<sup>3</sup>) and a surfactant [cetyltrimethylammonium chloride; CTAC] ( $1.0 \times 10^{-2}$  mol/dm<sup>3</sup>) has been investigated, and their properties were characterized by X-ray diffraction (XRD), Fourier transform infrared (FTIR), scanning and transmission electron microscopy (SEM and TEM),  $\text{N}_2$  and  $\text{H}_2\text{O}$  adsorption measurements, and thermogravimetric-differential thermal analyses (TG-DTA). The size and shape of the particles produced strongly depended on the concentration of the reactants and the aging temperature. Spherical calcium hydroxyapatite particles were precipitated only within a narrow concentration domain of reactants after aging at 100 °C for 3 h. The spherical calcium hydroxyapatite particles produced at  $[\text{CaSO}_4] = 2.0 \times 10^{-3}$  mol/dm<sup>3</sup> and  $[\text{NaH}_2\text{PO}_4] = 7.9 \times 10^{-4}$  mol/dm<sup>3</sup> were agglomerates of small platelet particles and were B-type carbonate hydroxyapatite in which 4.8 wt % of  $\text{CO}_3^{2-}$  ions are substituted for  $\text{PO}_4^{3-}$  ions. The results of chemical analysis and TG identified the formula of the particles as  $\text{Ca}_{8.5}\text{Na}_{1.5}(\text{PO}_4)_{5.4}(\text{CO}_3)_{0.8}(\text{OH})_{0.7}1.2\text{H}_2\text{O}$ . The texture and crystallinity of the spherical calcium hydroxyapatite particles were sustained up to 1000 °C, and the particles showed the selective adsorption of  $\text{H}_2\text{O}$  molecules. This selective adsorption was more pronounced after calcining the samples in air.

## Introduction

To produce high-quality materials, studies on the preparation and characterization of uniform, spherical, metal phosphate particles have been extensively carried out.<sup>1-5</sup> Recently, we investigated the formation and characterization of uniform spherical cobalt and nickel phosphate particles,<sup>6-8</sup> prepared by aging a solution containing  $\text{CoSO}_4$  or  $\text{NiSO}_4$  and  $\text{NaH}_2\text{PO}_4$  at 80 °C in the presence of urea and sodium dodecyl sulfate (SDS). These studies indicated that the cobalt phosphate particles possess thermally unstable slit-shaped micropores and exhibit a high selectivity for  $\text{H}_2\text{O}$  adsorption by the molecular sieve effects of these micropores.<sup>6,8</sup> On the other hand, it was found that, differing from the cobalt phosphate particles, the nickel phosphate particles are agglomerates of fine, primary, spherical particles with a high mesoporosity.<sup>7</sup>

Recently, calcium hydroxyapatite [ $\text{Ca}_{10}(\text{PO}_4)_6(\text{OH})_2$ , CaHAP] has attracted a great deal of attention due to its affinity to biopolymers such as proteins and enzymes and the fact that this material is a major inorganic crystalline constituent in human-calcified hard tissues

such as bone and teeth. Therefore, many studies have employed CaHAP with high-performance liquid chromatography (HPLC) for separating biopolymers.<sup>9-11</sup> Spherical CaHAP can be expected to attain a high separation efficiency with HPLC due to its large packing fraction. However, to our knowledge, spherical CaHAP has been produced only by a spray drying technique.<sup>12</sup> Therefore, development of a new technique for producing spherical CaHAP particles with a narrow size distribution from an aqueous solution phase is desired. In the current study, we extended our investigation on the preparation and characterization of metal phosphate particles obtained by a homogeneous precipitation method to produce spherical CaHAP. The spherical CaHAP particles obtained by aging a mixed solution of  $\text{CaSO}_4$ - $\text{NaH}_2\text{PO}_4$  in the presence of urea and a surfactant were characterized in terms of their structure, composition, crystallinity, specific surface area, and ultramicroporosity.

## Experimental Section

All the chemicals used were a guaranteed reagent grade from Wako Co. Ltd. and were used without further purification. Calcium phosphate particles were prepared using a solution of  $\text{CaSO}_4$ ,  $\text{NaH}_2\text{PO}_4$ , urea (1 mol/dm<sup>3</sup>), and CTAC ( $1.0 \times 10^{-2}$  mol/dm<sup>3</sup>) in a 20 cm<sup>3</sup> Teflon-lined screw-capped Pyrex test tube aged in a turbulent air circulation oven at 80 and 100 °C for 1 h to 6 days, using essentially the same recipe for

<sup>⊗</sup> Abstract published in *Advance ACS Abstracts*, November 15, 1994.

(1) Katsanis, E. P.; Matijević, E. *Colloids Surf.* **1982**, *5*, 43.

(2) Wilhelmy, R. B.; Patel, R. C.; Matijević, E. *Inorg. Chem.* **1985**, *24*, 3290.

(3) Ishikawa, T.; Matijević, E. *J. Colloid Interface Sci.* **1988**, *123*, 122.

(4) Wilhelmy, R. B.; Matijević, E. *Colloids Surf.* **1987**, *22*, 111.

(5) Springsteen, I. I.; Matijević, E. *Colloid Polym. Sci.* **1987**, *267*, 1007.

(6) Kandori, K.; Toshioka, M.; Nakashima, H.; Ishikawa, T. *Langmuir* **1993**, *9*, 1031.

(7) Kandori, K.; Nakashima, H.; Ishikawa, T. *J. Colloid Interface Sci.* **1993**, *160*, 499.

(8) Kandori, K.; Matsuda, E.; Yasukawa, A.; Ishikawa, T.; *Shikizai*, in press.

(9) Kawasaki, T.; Niikura, M.; Takahashi, S.; Kobayashi, W. *Biochem. Int.* **1986**, *13*, 969.

(10) Kawasaki, T.; Ikeda, K.; Takahashi, S.; Kuboki, Y. *Eur. J. Biochem.* **1986**, *155*, 249.

(11) Kawasaki, T.; Kobayashi, W.; Ikeda, K.; Takahashi, S.; Honma, H. *Eur. J. Biochem.* **1986**, *157*, 291.

(12) Itatani, K.; Takahashi, O.; Kishioka, A.; Kinoshita, M. *Gypsum Lime* **1988**, *213*, 19.

cobalt and nickel phosphate particle production.<sup>5-8</sup> The concentration of  $\text{CaSO}_4$  was varied from  $31.6 \times 10^{-5}$  to  $5 \times 10^{-3}$  mol/dm<sup>3</sup>. The concentration of  $\text{NaH}_2\text{PO}_4$  was varied from  $31.6 \times 10^{-5}$  to  $31.6 \times 10^{-3}$  mol/dm<sup>3</sup>. The precipitates produced were washed thoroughly with distilled water and finally dried in vacuo at room temperature for 16 h.

X-ray diffraction measurements were taken using a diffractometer (XRD, Rigaku UO-200B) using Cu K $\alpha$  radiation (30 kV, 15 mA). Infrared spectra of CaHAP in KBr pellets were measured using a Fourier transform infrared spectrometer (FTIR; Horiba FT-200). The  $\text{CO}_3^{2-}$  ion concentration in the particle was estimated using a calibration curve which was made using the intensity of the IR bands of the  $\text{CO}_3^{2-}$  ions of  $\text{CaCO}_3$  as a standard material. The accuracy of this method was  $\pm 0.2$  wt %. Additional IR spectra were recorded *in situ* using an FTIR spectrophotometer (Degilab FTS15E) with a PbSe detector having a high sensitivity in the near-IR region. The particles were pasted on a glass plate and were pretreated in a vacuum cell at temperatures varying from 25 to 400 °C for this measurement.

Ca and P contents of the particles were assayed respectively using inductively coupled plasma spectroscopy (ICP, Seiko SPS1200VR) and using the molybdenum blue method.<sup>13</sup> Scanning and transmission electron microscopy (SEM, JEOL JSM-840A, TEM; JEOL 1200) was used to ascertain the morphology of the particles. The adsorption isotherms of  $\text{N}_2$  were measured at liquid  $\text{N}_2$  temperature using a computerized volumetric apparatus constructed in our laboratory with the error of  $\pm 0.2$  wt %.<sup>14</sup> A computerized automatic gravimetric instrument designed in our laboratory was employed for determining the adsorption isotherms of  $\text{H}_2\text{O}$  at 25 °C, the sensitivity being  $10 \mu\text{g}$ .<sup>15</sup> Before any gas adsorption measurements were taken, the samples were pretreated at  $10^{-2}$  Pa at temperatures varying from 25 to 400 °C for 2 h. Before outgassing at 100 °C for 2 h, several samples were treated in air at temperatures varying from 200 to 1000 °C for 2 h. TG-DTA measurements were carried out with a thermobalance (Seiko TG-DTA 220) connected to a data station (SSC/5200H). Sensitivity of the equipment was determined to be  $\pm 0.2 \mu\text{g}$  for TG and  $\pm 0.06 \mu\text{V}$  for DTA.

## Results and Discussion

**Morphology of Precipitated Particles.** The size and shape of the particles strongly depended on the concentration of the reactants in the starting solution and aging temperature. Figure 1 gives the morphology of the precipitates at various concentrations of  $\text{CaSO}_4$  and  $\text{NaH}_2\text{PO}_4$  produced after aging at 80 and 100 °C. A precipitate was not obtained at concentrations of  $\text{CaSO}_4$  below  $1.0 \times 10^{-3}$  mol/dm<sup>3</sup>. It was seen that changing the aging temperature remarkably controlled the morphology of the precipitates. Platelet and needle aggregated particles were produced at 80 °C while the spherical particles appeared at 100 °C in addition to the platelet and needle aggregated particles. Typical TEM and SEM micrographs of platelet, needle aggregated and spherical particles are given in Figure 2. It must be noted that the spherical particles were produced only at 100 °C. The high-magnification SEM picture of the spherical particles in Figure 2E seems to indicate that these particles are formed by the aggregation of smaller platelet particles. Since the aim of this study is to develop a preparation method for spherical CaHAP particles, we employed the spherical particles formed at  $[\text{CaSO}_4] = 2.0 \times 10^{-3}$  mol/dm<sup>3</sup>,  $[\text{NaH}_2\text{PO}_4] = 7.9 \times$

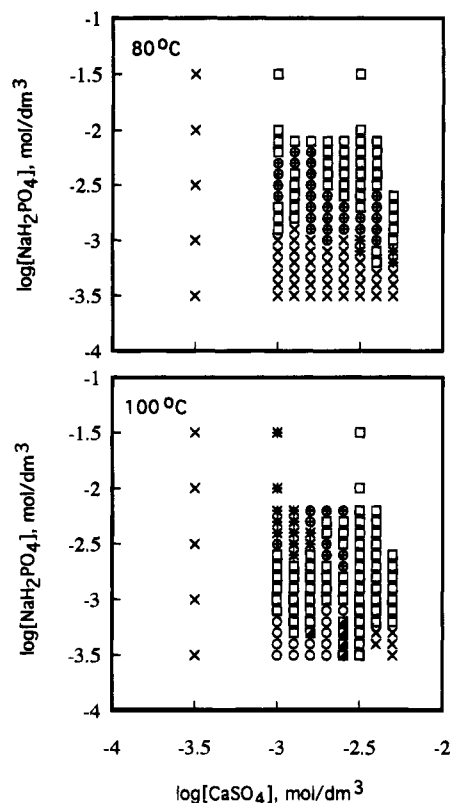


**Figure 1.** Concentration domains of solutions containing different concentrations of  $\text{CaSO}_4$  and  $\text{NaH}_2\text{PO}_4$  in the presence of urea ( $1 \text{ mol/dm}^3$ ) and CTAC ( $1.0 \times 10^{-2} \text{ mol/dm}^3$ ). Aging time was 3 h. (x) no precipitates, (\*) aggregated needles, (⊕) aggregated needle and platelets, (□) platelets, (○) spheres, (◻) spheres and platelets.

$10^{-4} \text{ mol/dm}^3$ , [urea] =  $1 \text{ mol/dm}^3$  and [CTAC] =  $1.0 \times 10^{-2} \text{ mol/dm}^3$  as displayed in Figure 2E for the following experiments.

**Characterization of Spherical Calcium Phosphate Particles.** The spherical particles produced exhibited the characteristic peaks of CaHAP in their XRD patterns as shown in Figure 3a. The spherical particles have a broad size distribution from 3 to  $15 \mu\text{m}$  and their average diameter is  $9.6 \pm 3.1 \mu\text{m}$ . It should be noted that the spherical particles are agglomerates of small platelet particles. The mean edge length of these platelet particles, assuming square plates, is estimated to be  $1.8 \times 2.0 \times 0.2 \mu\text{m}^3$ . The average crystallite sizes of the (300), (211), and (002) planes of the particles estimated from XRD patterns by using the Scherrer equation were 40, 57, and 47 nm, respectively. These values were not only smaller than the size of the spherical particles but also smaller than that of the agglomerated platelet particles, indicating that the particles are polycrystalline. Figure 4 shows the change of pH during preparation of the spherical CaHAP particles aged at 100 °C. The pH steeply increased up to 9.5 within 3 h of aging through the decomposition of urea and became almost constant at 9.8 after aging for 4 h. This fact corresponds with the fact that CaHAP

(16) Monma, H. *Shokubai* **1985**, *27*, 237.

(17) Bell, L. B.; Blacks, C. A. *Soil Sci. Soc. Am. Proc.* **1970**, *34*, 583.

(18) Makishima, A.; Aoki, H. *Bioceramics*; Yamaguchi, T., Yanagida, H., Eds.; Gihodo: 1984.

(19) Brown, W. E.; Mathew, M.; Tung, M. S. *Prog. Cryst. Growth Charact.* **1981**, *4*, 59.

(20) Monma, H. *Kogyozairyo* **1980**, *28*, 97.

(13) Boltz, D. F., Ed. *Colorimetric Determination of Nonmetals*, 2nd ed.; 1987; p 342 (1987).

(14) Kondo, S.; Fujiwara, H.; Amano, E. *Shikizai* **1980**, *53*, 697.

(15) Naoki, K.; Amano, E.; Kondo, S. *Memories Osaka Univ. Educ.* **1977**, *26*, 1.

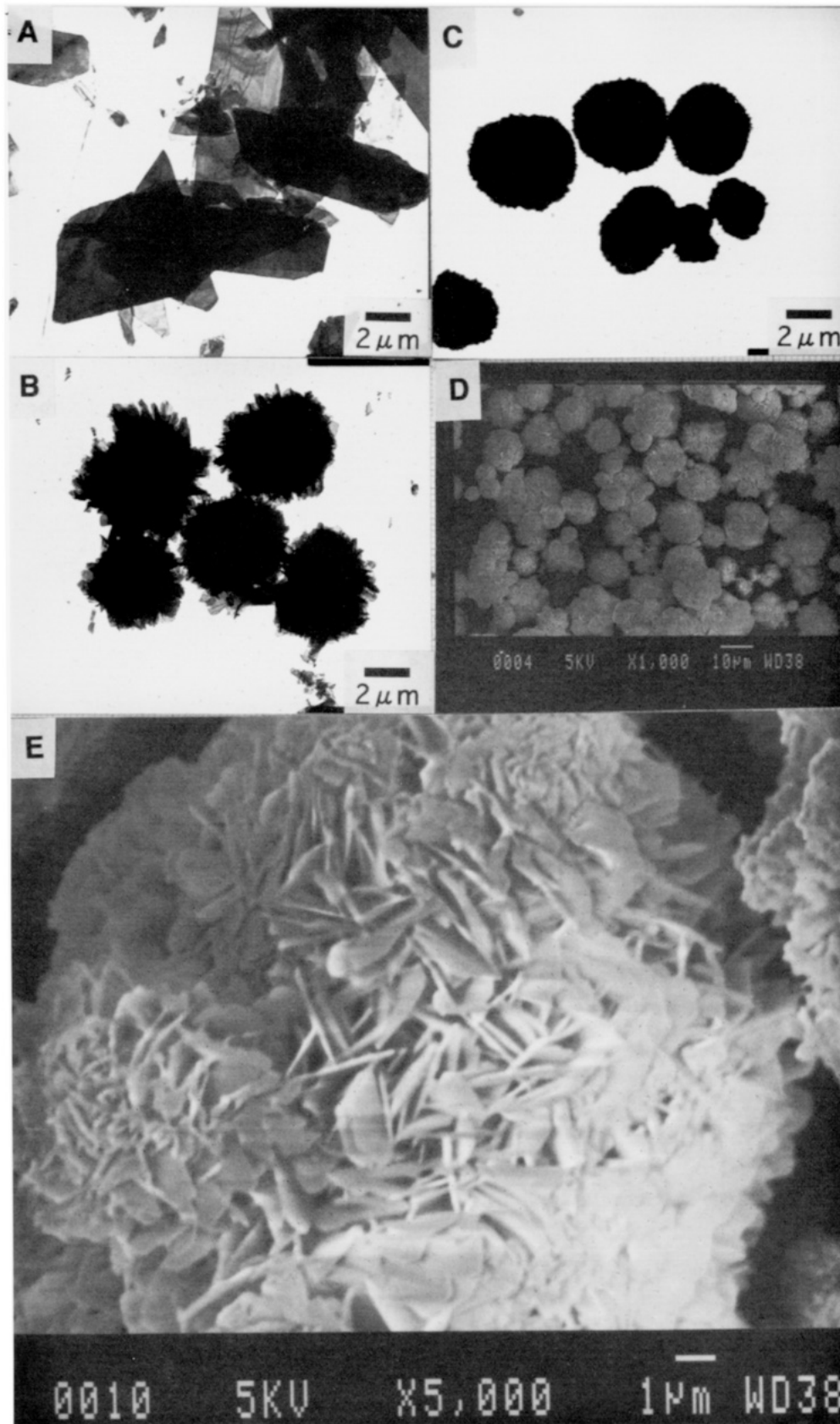


**Figure 2.** Electron micrographs of platelets, aggregated needles and spherical precipitates formed under fixed concentration of urea ( $1 \text{ mol/dm}^3$ ) and CTAC ( $1.0 \times 10^{-2} \text{ mol/dm}^3$ ). Aging temperature was  $100^\circ\text{C}$ . (A) Platelets precipitated at  $[\text{CaSO}_4] = 3.2 \times 10^{-3} \text{ mol/dm}^3$  and  $[\text{NaH}_2\text{PO}_4] = 6.3 \times 10^{-3} \text{ mol/dm}^3$ . (B) Aggregated needles precipitated at  $[\text{CaSO}_4] = 1.3 \times 10^{-3} \text{ mol/dm}^3$  and  $[\text{NaH}_2\text{PO}_4] = 4.0 \times 10^{-3} \text{ mol/dm}^3$ . (C) Spheres precipitated at  $[\text{CaSO}_4] = 2.0 \times 10^{-3} \text{ mol/dm}^3$  and  $[\text{NaH}_2\text{PO}_4] = 7.9 \times 10^{-4} \text{ mol/dm}^3$ . (D) SEM micrograph of sample (C). (E) High magnification SEM micrograph of sample (C).

particles are produced at a  $\text{pH} > 8.0$  as reported by many investigators.<sup>16-20</sup> Bosky and Posner, in their study of the precipitation of calcium phosphates from

the reaction of  $\text{Ca}^{2+}$  and  $\text{PO}_4^{3-}$  ions in aqueous media, reported that CaHAP is precipitated directly from solution when the product of the molar concentrations

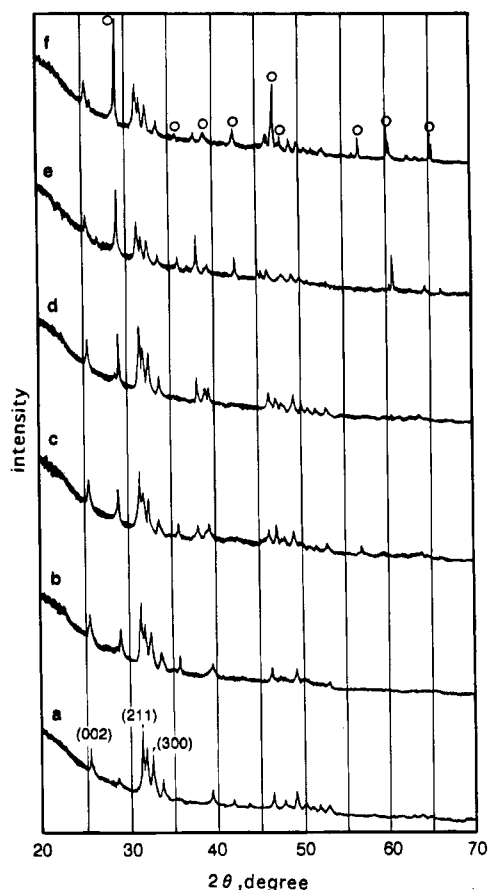


**Figure 3.** XRD patterns of spherical calcium phosphate particles precipitated at various aging periods. Aging temperature was 100 °C.  $[\text{CaSO}_4] = 2.0 \times 10^{-3} \text{ mol/dm}^3$ ,  $[\text{NaH}_2\text{PO}_4] = 7.9 \times 10^{-4} \text{ mol/dm}^3$ ,  $[\text{urea}] = 1 \text{ mol/dm}^3$ , and  $[\text{CTAC}] = 1.0 \times 10^{-2} \text{ mol/dm}^3$ . Aging periods: (a) 3 h, (b) 6 h, (c) 1 day, (d) 2 days, (e) 4 days, (f) 6 days. The open circle represents the characteristic peaks of  $\text{CaCO}_3$  (calcite).

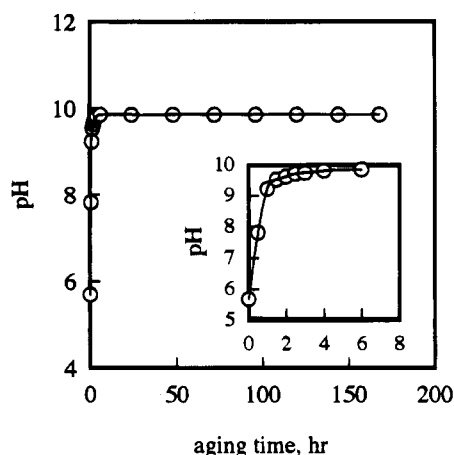


**Figure 4.** Change in the solution pH with aging time.  $[\text{CaSO}_4] = 2.0 \times 10^{-3} \text{ mol/dm}^3$ ,  $[\text{NaH}_2\text{PO}_4] = 7.9 \times 10^{-4} \text{ mol/dm}^3$ ,  $[\text{urea}] = 1 \text{ mol/dm}^3$  and  $[\text{CTAC}] = 1.0 \times 10^{-2} \text{ mol/dm}^3$ .

of  $\text{Ca}^{2+}$  and  $\text{PO}_4^{3-}$  ions,  $[\text{Ca}^{2+}][\text{PO}_4^{3-}]$ , ranges from  $0.25 \times 10^{-6}$  to  $1.67 \times 10^{-6} \text{ (mol/dm}^3)^2$ .<sup>21</sup> The product of  $[\text{Ca}^{2+}][\text{PO}_4^{3-}]$  in the present study is  $1.58 \times 10^{-6} \text{ (mol/dm}^3)^2$ , which is consistent with the results of Bosky and Posner. Also Aoki and Kato found that CaHAP particles are formed at  $\text{pH} > 6.0$  and 100 °C,<sup>22</sup> supporting our observations.

In the course of studying the formation mechanism of the spherical CaHAP particles, SEM studies were

performed on the samples that had precipitated after various aging periods. The photos are shown in Figure 5. No precipitation was observed when the aging time was less than 40 min. After aging for 1 h, the spherical particles in the 3–15  $\mu\text{m}$  diameter range appeared abruptly without observation of fine primary particles and maintained their shape and size until 3 h of aging had passed. This fact implies that the primary particles aggregated rapidly reducing the interfacial free energy. After aging for 6 h, however, needlelike and cubic particles appeared. Comparing to the XRD patterns of these samples as shown in Figure 3b–f, these needlelike and cubic particles can be assigned to  $\text{CaCO}_3$  (calcite). The characteristic peaks of  $\text{CaCO}_3$  marked by the open circles emerged after the sample had been aged for 4 h. Since the decomposition of urea produces  $\text{CO}_2$ , it is understandable that  $\text{CaCO}_3$  particles are formed by the reaction of dissolved  $\text{CO}_2$  in basic medium with  $\text{Ca}^{2+}$  ions dissolved from the precipitated spherical CaHAP particles and/or with residual  $\text{Ca}^{2+}$  ions. Therefore, particular attention should be given to the effect of  $\text{CO}_2$  when forming CaHAP.

It is known that there are two kinds of biological apatites containing  $\text{CO}_3^{2-}$  ions in different sites;<sup>23–25</sup> one is the A-type carbonate hydroxyapatite (CAP) in which  $\text{CO}_3^{2-}$  ions are substituted for  $\text{OH}^-$  ions, and the other is the B-type CAP in which  $\text{CO}_3^{2-}$  ions are substituted for  $\text{PO}_4^{3-}$  ions. The IR spectra of CaHAP in KBr after calcination of samples in air at 25, 100, 200, 400, 600, 800, and 1000 °C are shown in Figure 6. The spectra contain the 1035, 960, 603, and 565  $\text{cm}^{-1}$  bands of  $\text{PO}_4^{3-}$  ions and the 1458, 1421, and 873  $\text{cm}^{-1}$  bands of  $\text{CO}_3^{2-}$  ions along with a broad peak of adsorbed water centered at 3400  $\text{cm}^{-1}$ . By increasing the pretreatment temperature, the intensity of the bands of the  $\text{CO}_3^{2-}$  ions decreased, and these bands completely disappeared with heat treatment at 1000 °C. Since these three bands of the  $\text{CO}_3^{2-}$  ions are characteristic to the B-type CAP,<sup>26</sup> the present synthetic CaHAP has been assigned to the B-type CAP.

TG-DTA curves of the spherical CaHAP particles are shown in Figure 7. Weight loss is observed up to 250 °C with a small endothermic peak in DTA, implying the elimination of adsorbed water. Furthermore, the weight loss continues until 1000 °C with a substantial weight loss at 635–675 °C accompanied by many endothermic peaks. Comparing the TG curve to the IR spectra in Figure 6, this weight loss of 7 wt % from 250 to 1000 °C is consistent with the elimination of  $\text{CO}_3^{2-}$  ions and bound water. It has been reported that the composition of B-type CAP is  $\text{Ca}_{10-x}\text{Na}_x(\text{PO}_4)_{6-y}(\text{CO}_3)_{4y/3}(\text{OH})_{2-x+y/3}$ .<sup>23</sup> The carbonate content in the spherical particles used in the present study has been estimated to be 4.8 wt % by FTIR measurement in a KBr pellet. Also, the calcium to phosphorus molar ratio of the particles was calculated to be 1.59. Because the difference between the weight loss of 7 wt % and carbonate content of 4.8 wt % is the bound water, the formula of this CaHAP

(21) Bosky, A. L.; Posner, A. L. *J. Phys. Chem.* **1976**, *80*, 40.

(22) Aoki, H.; Kato, K. *Shika Rikogaku Zasshi* **1973**, *14*, 36.

(23) Miyake, M.; Watanabe, K.; Nagayama, Y.; Hasegawa, H.; Suzuki, T. *J. Chem. Soc., Faraday Trans.* **1990**, *86*, 2303.

(24) Zapanta-LeGeros, R. *Nature* **1965**, *206*, 403.

(25) Ioku, K.; Yoshimura, M.; Munemiya, S. *Nippon Kagaku Kaishi* **1985**, 1565.

(26) Roy, D. M.; Eysel, W.; Dinger, D. *Mater. Res. Bull.* **1974**, *9*, 35.

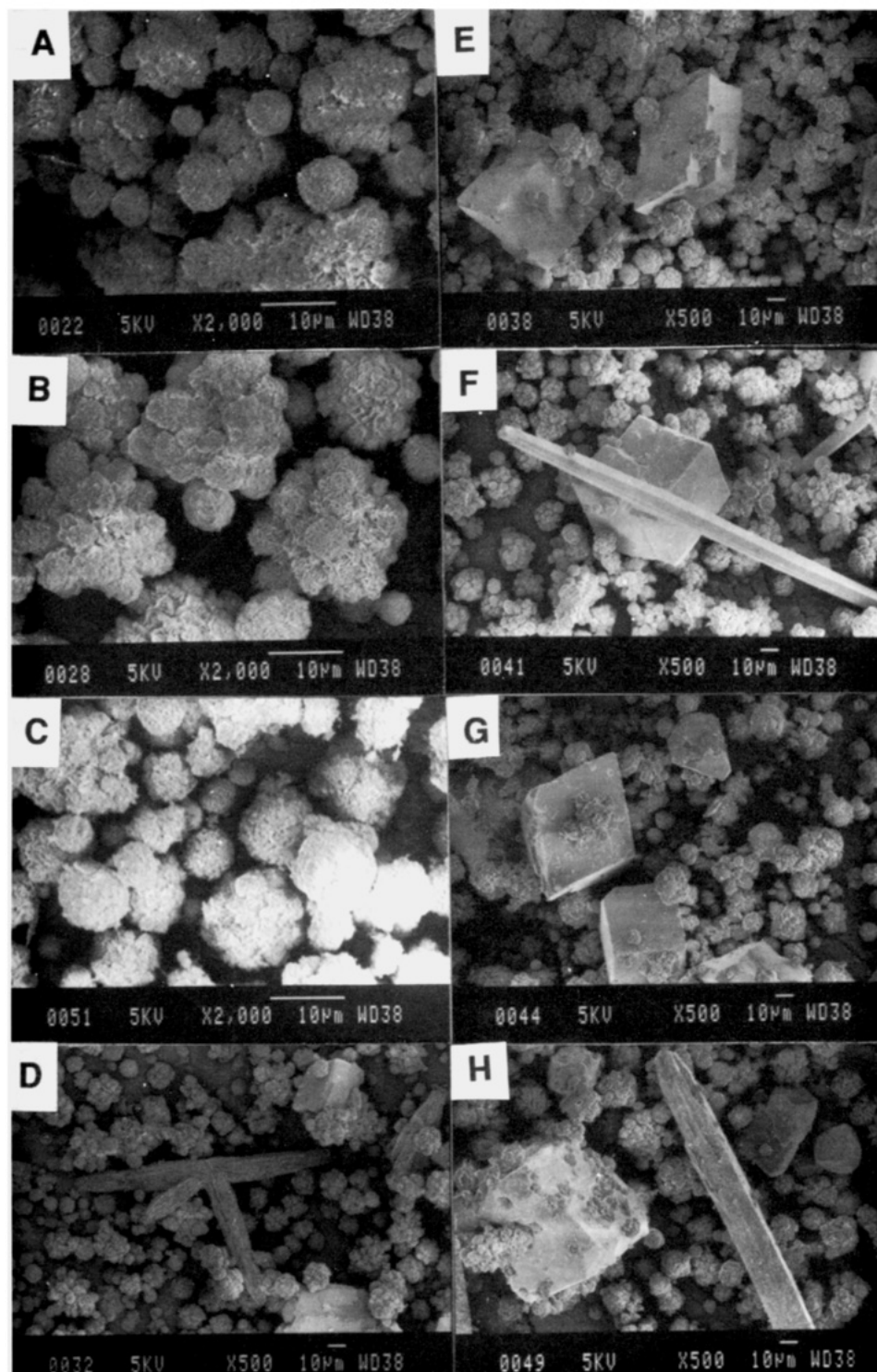


**Figure 5.** SEM micrographs of precipitates formed at various aging periods. Aging temperature was 100 °C.  $[\text{CaSO}_4] = 2.0 \times 10^{-3} \text{ mol/dm}^3$ ,  $[\text{NaH}_2\text{PO}_4] = 7.9 \times 10^{-4} \text{ mol/dm}^3$ ,  $[\text{urea}] = 1 \text{ mol/dm}^3$  and  $[\text{CTAC}] = 1.0 \times 10^{-2} \text{ mol/dm}^3$ . Aging periods: (A) 1 h, (B) 2 h, (C) 3 h, (D) 6 h, (E) 1 day, (F) 2 days, (G) 4 days, (H) 6 days.

specimen could be given as  $\text{Ca}_{8.5}\text{Na}_{1.5}(\text{PO}_4)_{5.4}(\text{CO}_3)_{0.8}(\text{OH})_{0.7} \cdot 1.2\text{H}_2\text{O}$ .

The morphology and crystal structure of the spherical CaHAP particles were sustained up to 1000 °C, suggesting a high thermal stability of the CaHAP. It can be seen from Figure 6 that a sharp peak at  $3568 \text{ cm}^{-1}$  increased in intensity with increasing calcination temperature in air. Ishikawa et al. have assigned the peak at  $3570 \text{ cm}^{-1}$  to the lattice  $\text{OH}^-$  ions in the CaHAP

particles.<sup>27</sup> Hence, the  $3568 \text{ cm}^{-1}$  band can be presumed to be of the same origin. For confirmation, we measured *in situ* IR spectra of the spherical CaHAP particles pasted on a glass plate set in a vacuum cell, and a hydrogen–deuterium isotope exchange was carried out with five cycles of adsorption of heavy water into the sample at  $1.33 \times 10^{-3} \text{ Pa}$  and 25 °C for 5 min. From this H–D isotope exchange, the  $3568\text{-cm}^{-1}$  band slowly changed to a band at  $2630 \text{ cm}^{-1}$ . The agreement of the isotope ratio of this band ( $3568/2630 = 1.357$ ) to the theoretical isotope ratio (1.374) provides evidence that

(27) Ishikawa, T.; Wakamura, M.; Kondo, S. *Langmuir* 1989, 5, 140.

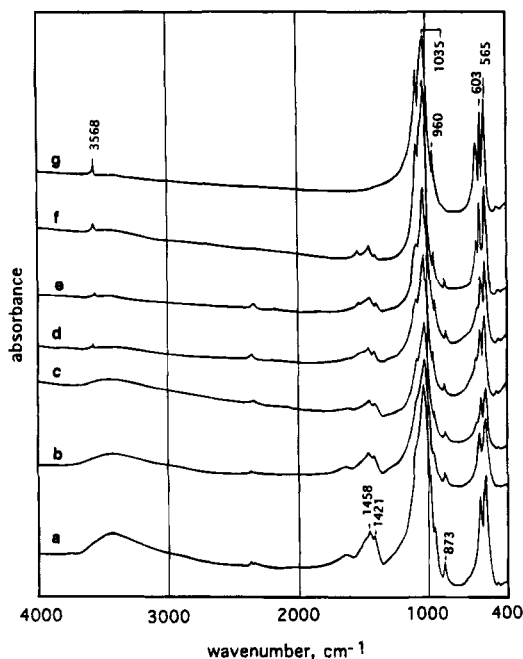


**Figure 6.** FTIR spectra of spherical calcium hydroxyapatite particles calcined at various temperatures in air for 2 h. Pretreatment temperature (°C): (a) 25, (b) 100, (c) 200, (d) 400, (e) 600, (f) 800, (g) 1000.

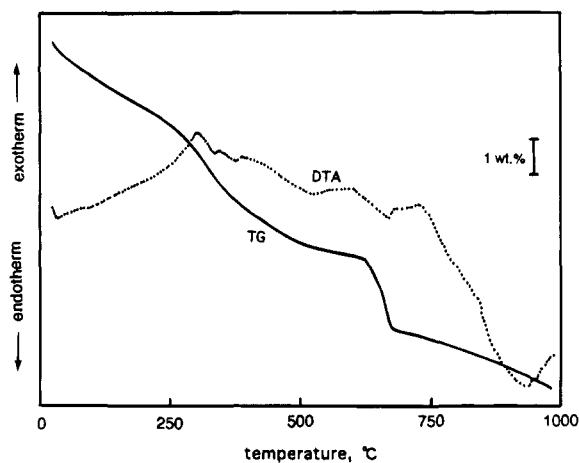


**Figure 7.** TG-DTA curves of spherical calcium hydroxyapatite particles.  $[\text{CaSO}_4] = 2.0 \times 10^{-3} \text{ mol/dm}^3$ ,  $[\text{NaH}_2\text{PO}_4] = 7.9 \times 10^{-4} \text{ mol/dm}^3$ ,  $[\text{urea}] = 1 \text{ mol/dm}^3$ , and  $[\text{CTAC}] = 1.0 \times 10^{-2} \text{ mol/dm}^3$ .

the 3568- $\text{cm}^{-1}$  band corresponds to the lattice  $\text{OH}^-$  ions.

We found in previous work that cobalt phosphate particles have slit-shape micropores and adsorb  $\text{H}_2\text{O}$  molecules selectively over  $\text{N}_2$  molecules.<sup>6</sup> Therefore, we were interested to know whether the spherical CaHAP particles produced in this study exhibit a similar adsorption selectivity or not. To determine this, we performed adsorption experiments with  $\text{N}_2$  and  $\text{H}_2\text{O}$ . Type II isotherms of the BDDT classification<sup>28</sup> were obtained for both adsorptive molecules. Figure 8 displays the typical adsorption isotherms of  $\text{N}_2$  for the particles, pretreated at 25, 50, and 150 °C in vacuo and 200 and 600 °C in air, and their pore-size distribution curves computed from these isotherms using the Cranston-Inkley method, respectively.<sup>29</sup> The steep increase of the

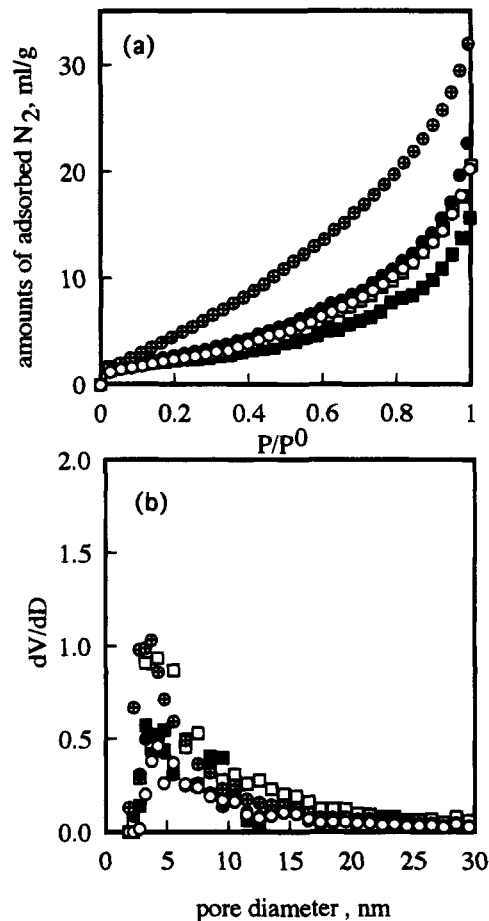


**Figure 8.** Adsorption isotherms of  $\text{N}_2$  (a) and pore-size distribution curves (b) for spherical hydroxyapatite particles pretreated at various conditions. Pretreatment temperature: (○), 25, (⊕), 50, (●), 150, (□), 200, (■), 600 °C, (○, ⊕, ●) in vacuo, (□, ■) in air.

adsorption isotherms of  $\text{N}_2$  at higher relative pressure indicates the existence of macropores.<sup>30</sup> Figure 8b also leads us to conclude that there are a few mesopores of diameter ranging from 2 to 20 nm, but no micropores have been produced with any pretreatment conditions. Since the specific surface areas measured by the  $\text{N}_2$  BET method are in fair agreement with the specific surface area estimated by the size of platelet particles as will be shown in the next paragraph, these meso- and macropores seem to be produced mainly by the interstices of agglomerated platelet particles. To quantitatively investigate the microporosity of the particles, we evaluated the specific surface areas of the particles from the adsorption isotherms of  $\text{N}_2$  and  $\text{H}_2\text{O}$  (abbreviated respectively as  $S_n$  and  $S_w$ ) by fitting the data to the BET equation.<sup>30</sup> In this calculation, we assumed the cross-sectional areas of  $\text{N}_2$  and  $\text{H}_2\text{O}$  molecules to be 0.162 and 0.108  $\text{nm}^2$ , respectively.<sup>30</sup> The obtained  $S_w$ ,  $S_n$ , and  $S_w/S_n$  ratios are plotted in Figure 9 as a function of the pretreatment temperature.

The  $S_n$  values of the particles pretreated in vacuum ranged from 9.0 to 25.8  $\text{m}^2/\text{g}$  and show a maximum at a pretreatment temperature of 50 °C. These values are much larger than the specific surface area of 0.1  $\text{m}^2/\text{g}$  expected for spherical particles but are close to that of

(28) Brunauer, S.; Deming, L. S.; Deming, S. W.; Teller, E. *J. Am. Chem. Soc.* **1940**, *62*, 1723.

(29) Cranston, R. W.; Inkley, F. A. *Adv. Catal.* **1957**, *9*, 143.

(30) Lowell, S.; Shields, J. E. *Powder Surface Area and Porosity*, 2nd ed.; Powder Technology Series: Chapman and Hall: London, 1979.

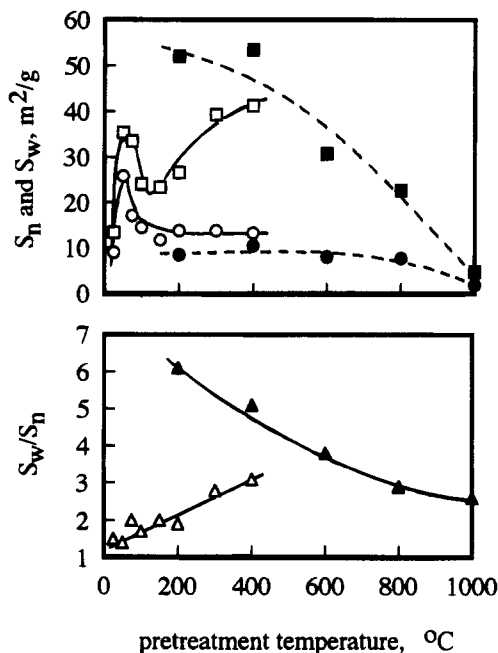


**Figure 9.** Plots of  $S_n$  and  $S_w$  (upper) and  $S_w/S_n$  ratio (lower) vs pretreatment temperature for spherical calcium hydroxyapatite particles. ( $\circ$ ,  $\bullet$ )  $S_n$ , ( $\square$ ,  $\blacksquare$ )  $S_w$ , ( $\triangle$ ,  $\blacktriangle$ )  $S_w/S_n$ , ( $\circ$ ,  $\square$ ,  $\triangle$ ) in vacuo, ( $\bullet$ ,  $\blacksquare$ ,  $\blacktriangle$ ) in air.

the  $4.2 \text{ m}^2/\text{g}$  of platelet particles which were estimated from their mean particle sizes assuming the density of CaHAP to be  $3.16 \text{ g}/\text{cm}^3$ . This is clear evidence that the spherical CaHAP particles are agglomerates of the small platelet particles as ascertained by the SEM and XRD measurements described before. A similar maximum is observed for the  $S_w$  values when aged at  $50 \text{ }^\circ\text{C}$ .

However, the  $S_w$  values are larger than  $S_n$  values and increase above  $150 \text{ }^\circ\text{C}$ . Another interesting finding is that the  $S_w/S_n$  ratio gradually increased with elevating pretreatment temperature from  $25$  to  $400 \text{ }^\circ\text{C}$ . Since the  $S_w/S_n$  ratio is a measure of the number of ultramicropores into which can take  $\text{H}_2\text{O}$  molecules but not  $\text{N}_2$  ones, this result indicates that the formation of ultramicropores in the small platelet particles is enhanced by an increase in the pretreatment temperature in vacuo. The rod-shaped CaHAP particles with dimensions of  $24 \times 72 \text{ nm}^2$  that were produced by aging the precipitates from a reaction of  $\text{Ca}(\text{OH})_2$  and  $\text{H}_3\text{PO}_4$  have no such selectivity.<sup>27</sup> More pronounced selectivity of  $\text{H}_2\text{O}$  adsorption was observed for the particles calcined in air as shown in Figure 9. The  $S_w/S_n$  ratio of 6.1 when pretreated at  $200 \text{ }^\circ\text{C}$  decreased to 2.6 with increasing calcination temperature up to  $1000 \text{ }^\circ\text{C}$ . This large  $S_w/S_n$  ratio implies that the formation of ultramicropores is enhanced by calcination in air. The reduction of the  $S_w/S_n$  ratio would be due to pore closure of ultramicropores by sintering. Because the  $S_n$  values represent the platelet particles as described before, it seems reasonable to consider that the ultramicropores were produced in each platelet particle. Here it should be restated that the highest ultramicroporosity is obtained for the spherical CaHAP particles by calcining in air at  $200 \text{ }^\circ\text{C}$ . Owing to this characteristic ultramicroporosity, the spherical CaHAP particles could be used in applications such as adsorbents, catalyst carriers, fillers, etc.

**Acknowledgment.** The authors thank Dr. Yoshihira Okanda and Mr. Masao Fukusumi of Osaka Municipal Technical Research Institute for help with the TEM observations.

CM9402616